

BORON ADSORPTION ON MODIFIED ZEOLITES: EFFECT OF MODIFIER AND SOURCE OF WATER

Adsorción de boro en zeolitas modificadas: efecto del modificador y la fuente de agua

Alicia Amairani FLORES DÍAZ¹, Martha Alicia VELÁZQUEZ MACHUCA^{1*},
Adriana MEDINA RAMÍREZ², José Luis MONTAÑEZ SOTO¹,
José VENEGAS GONZÁLEZ¹ and José Luis PIMENTEL EQUIHUA³

¹ Centro Interdisciplinario de Investigación para el Desarrollo Integral Regional-Unidad Michoacán, Instituto Politécnico Nacional, Justo Sierra 28, 59510 Jiquilpan, Michoacán, México.

² Departamento de Ingeniería Química, Universidad de Guanajuato, Noria Alta s/n, 36050 Guanajuato, México.

³ Colegio de Postgraduados-Campus Montecillo, km 36.5 carretera México-Texcoco, 56230 Montecillo, México.

*Author for correspondence: mvelazquezm@ipn.mx

(Received: June 2021; Accepted: May 2023)

Key words: LTL zeolite, FAU X zeolite, NiCl₂, FeCl₃, APS.

ABSTRACT

The removal of boron from drinking water is a concern in various parts of the world due to the toxic effects of this metalloid in high concentrations. In this paper, zeolites LTL and FAU X were synthesized and modified with salts of nickel (NiCl₂), iron (FeCl₃), and aminopropyltriethoxysilane (APS) in order to promote their affinity for boron species present in aqueous systems. The adsorption capacity of modified zeolites for boron was evaluated in a synthetic boron solution and with groundwater samples for human use. The effect of the pH and zeolite dose was studied in adsorption tests using groundwater. The modified zeolites were characterized by X-ray diffraction, scanning electron microscopy, transmission electron microscopy, nitrogen physisorption, and Fourier-transform infrared spectroscopy. Results indicated that the modification of zeolites favors affinity for boron species. The highest adsorption capacity of boron on zeolites was achieved in the synthetic solution. The adsorption capacity of the modified zeolites depended on the pH, the electrical conductivity, the modifying agent, the zeolitic structure, and the dose of adsorbent. The zeolitic structure-modifying agent interaction was decisive for boron adsorption capacity, with LTL-Ni zeolite being the best-performing adsorbent, thanks to its textural properties and nickel's ability to form complexes with boron species.

Palabras clave: zeolita LTL, zeolita FAU X, NiCl₂, FeCl₃, APS.

RESUMEN

La eliminación del boro en agua para consumo humano es una preocupación en diversas partes del mundo debido a sus efectos tóxicos en altas concentraciones. En el presente trabajo se sintetizaron zeolitas LTL y FAU X y se modificaron con sales de níquel (NiCl₂), de hierro (FeCl₃) y aminopropiltrióxido de silano (APS) a fin de promover su afinidad por especies de boro presentes en sistemas acuosos. La capacidad de adsorción de boro sobre las zeolitas modificadas se evaluó en una solución de boro sintética y con muestras de agua

subterránea para uso humano. El efecto del pH y la dosis de zeolita se estudiaron en las pruebas de adsorción utilizando agua subterránea. Las zeolitas modificadas fueron caracterizadas mediante difracción de rayos X, microscopia electrónica de barrido, microscopia electrónica de transmisión, fisisorción de nitrógeno y espectroscopia de infrarrojos por transformada de Fourier. Los resultados indicaron que la modificación de las zeolitas favorece la afinidad por las especies de boro. La mayor capacidad de adsorción de boro sobre las zeolitas se alcanzó en la solución sintética. La capacidad de adsorción de las zeolitas modificadas dependió del pH, la conductividad eléctrica, el agente modificante, la estructura zeolítica y la dosis de adsorbente. La interacción estructura zeolítica-agente modificante fue decisiva para la capacidad de adsorción de boro, siendo la zeolita LTL-Ni el adsorbente con mejor desempeño, gracias a sus propiedades texturales y a la habilidad del níquel para formar complejos con especies de boro.

INTRODUCTION

Boron is an element required for the development of plants, animals and humans (Khaliq et al. 2018); however, higher concentrations can induce adverse effects on human health and biota. Particularly, it has been reported (Weir and Fisher 1972, Price et al. 1996, Hilal et al. 2011) that high concentrations generate reproductive toxicity in animals (rats, mice, rabbits). Although negative effects on human reproduction have not been found (Bolt et al. 2020), boron causes nausea, diarrhea, headache, kidney damage, and even death due to circulatory collapse (Nasef et al. 2014). Recently an *in vitro* study reported that a high boron dose promotes the transforming activity of nontumorigenic cells (Xu et al. 2020). The World Health Organization (WHO 2017) has established a critical limit of 2.4 mg/L for boron concentration in human drinking water, while for irrigation waters the critical levels vary from 0.3 to 3 mg/L depending on the sensitivity of the crops (Ayers and Westcot 1989, Landi et al. 2019). The presence of high concentrations of boron has been detected in groundwater, wastewater, and rivers (Koç 2007, Xu et al. 2010, Velázquez et al. 2011, Palmucci and Rusi 2014). This situation reduces the availability of water resources, which is crucial due to water scarcity in different regions of the world (Boretti and Rosa 2019).

Among the techniques reported for boron removal, adsorption is a simple process whose effectiveness depends on the selectivity of the adsorbent, the boron concentration, and pH (Ezechi et al. 2012). These characteristics determine the usefulness of adsorption for low boron concentrations (Guan et al. 2016, Weidner and Ciesielczyk 2019). In this sense, different materials have been evaluated as adsorbents of boron: resins, alumina, activated carbon, low-cost sorbents, oxides and hydroxides, mesoporous silica,

layered double hydroxides, among others (Ezechi et al. 2012, Theiss et al. 2013, Guan et al. 2016).

Zeolites are highly crystalline aluminosilicates with a nanoporous structure which makes them useful for gas separation as catalysts, ionic exchangers, and adsorbents (Byrappa and Yoshimura 2013), characteristics that diversify their application in industrial processes, agriculture, and environmental protection. The adsorption properties of zeolites depend on their framework type, Si/Al ratio, and chemical surface (Yu and Han 2015). This last one is decisive for the anion or neutral species removal because the zeolites require to be modified in order to increase their affinity for these chemical species.

Diverse studies have evaluated the adsorption capacity of anions on modified zeolites, varying the zeolite type, the adsorption conditions and the type of modifier for nitrates (Schick et al. 2010, Batubara et al. 2018), molybdates (Verbinnen et al. 2012), cromates (Barquist and Larsen 2010), arsenates and arsenites (Medina-Ramírez et al. 2013, 2019, Noroozifar et al. 2014) and selenium oxyanions (Jevtić et al. 2014).

Boron adsorption on modified zeolites has been studied on HDTMA-Br modified clinoptilolite reaching a removal efficiency higher than 60 % at a pH of 8.5 (Demirçivi and Nasün-Saygili 2010). Dionisiou et al. (2013) reported a boron removal of 24 % at a pH of 9.5. Kluczka et al. (2013) reported the boron adsorption on ZrO₂ modified-clinoptilolite; they evaluated the effect of pH, temperature, dose, concentration, and adsorption time, achieving a boron removal of 75 %.

Chen et al. (2020) studied the boron removal on magnetite nanoparticles and they found evidence of the formation of a Fe-O-B bond that enhances the boron adsorption. Jalali et al. (2016) evaluated modified FeCl₃ mineral and organic sorbents for boron adsorption; their best results were obtained using the

modified organic sorbent. Additionally, the formation of a nickel complex with boric acid and polyborates was documented by Graff et al. (2017), who showed the thermodynamic stability of the complex. These results suggest the viability of evaluating nickel as a modifier of sorbent for boron removal.

In addition, the modification of nanoparticles by aminosilanes has been reported as an efficient strategy to improve the adsorption of chromate ions (Hozhabr et al. 2015). For these reasons, the effect of nickel chloride, ferric chloride, and aminopropyltriethoxysilane (APS) as modifier agents of LTL and FAU X zeolites, was studied in the present work, and the boron removal capacity of the modified zeolites was evaluated. The zeolites were chosen considering the difference in their topology and the pore channel systems, where FAU X is characterized by three-dimensional channel systems while LTL poses unidimensional channel systems, characteristics that influence the diffusion for modification and adsorption processes. Additionally, the boron adsorption capacity of the modified zeolites was evaluated using groundwater samples and their performance was compared using a synthetic boron solution. The groundwater samples were obtained from a well located in the geothermal area of Ixtlán de los Hervores, Michoacán, Mexico. In this area, the groundwater contains high concentrations of boron, a condition associated to geothermal activity, being the zone near the Ixtlán geyser where the highest boron concentration (11.268 mg/L) has been detected (Velázquez et al. 2011).

MATERIALS AND METHODS

Materials

For zeolite synthesis, sodium aluminate ($\text{Al}_2\text{Na}_2\text{O}_4$, 99 %) and aluminum hydroxide ($\text{Al}(\text{OH})_3$, 99 %) were used as alumina precursors; Ludox HS-40 as silica precursor, sodium hydroxide (NaOH, 97 %) and potassium hydroxide (KOH, 90 %) as mineralizing agents, and deionized water as reaction media. Salts of nickel (NiCl_2 , 99.9 %) and iron (FeCl_3 , 99.9 %), as well as 3-APS (99 %) were used as modifying agents of the zeolites. Boric acid (H_3BO_3 , 99.5 %) was used for the synthetic boron solution. All reagents were purchased from Sigma Aldrich.

Synthesis and modification of the zeolites

The faujasite type X and LTL (Linde Type-L) zeolites were synthesized by the hydrothermal method. The LTL zeolite was obtained following the procedure reported by Mintova (2016). Briefly, an alumina

solution of molar composition 0.01096 M $\text{Al}(\text{OH})_3$, 0.06896 M KOH and 0.5277 M H_2O was prepared. Afterwards, a silica solution of molar composition 0.1142 M SiO_2 , 0.034 M KOH and 0.4861 M H_2O was obtained. The alumina solution was added drop to drop to the silica solution under stirring. The obtained gel was aged at room temperature for 40 h. Subsequently, the slurry was transferred to a Parr Teflon-lined stainless-steel autoclave and it was submitted to crystallization at 170 °C for 20 h. The final product was recovered by centrifugation, and it was washed with deionized water. The solid was dried at 60 °C for 24 h.

On the other hand, the X zeolite was synthesized according to the procedure described by Lechert and Staelin (2001). First, an alumina solution of molar composition 0.0022 M Al_2O_3 , 0.0146 M Na_2O and 0.5733 M H_2O was prepared, then a silica solution was obtained from a molar composition of 0.0188 M SiO_2 , 0.0175 M Na_2O and 0.694 M H_2O . Subsequently, the alumina solution was slowly added to the silica solution. The slurry was kept under stirring for 20 min. Afterwards, the suspension was transferred to a Parr Teflon-lined stainless-steel autoclave and it was submitted to crystallization at 90 °C for 8 h. The final product was recovered, washed with deionized water and dried at 100 °C for 6 h.

Modification of the LTL and X zeolite was carried out by chemical exchange. For this purpose, three modifying solutions with a 10 mM concentration were prepared by dissolution of nickel chloride, ferric chloride and APS in deionized water. The zeolite (LTL or X) was added to the modifying solution, and it was kept under stirring for 24 h at 40 °C. The modified zeolite was recovered, washed and dried at 100 °C for 12 h. Six modified zeolites were obtained, which resulted from modifying zeolites X and LTL, each one with three modifiers: NiCl_2 , FeCl_3 and 3-APS. The label of each sample corresponded to the name of the zeolite followed by the metallic ion, for instance LTL-Ni. For zeolites modified with APS, the zeolite name was followed by APS.

Groundwater samples collection and analysis

The groundwater samples were obtained from a well within the geothermal area of Ixtlán de los Hervores, Michoacán, Mexico (20°10'05" N, 102°22'52" W; Fig. 1). This well is used as a source of drinking water and it has an average boron concentration of 5.5 mg/L. The water samples were directly collected from the well in polypropylene bottles previously washed with a solution of sulfuric acid and deionized water. During the sampling, pH, electric

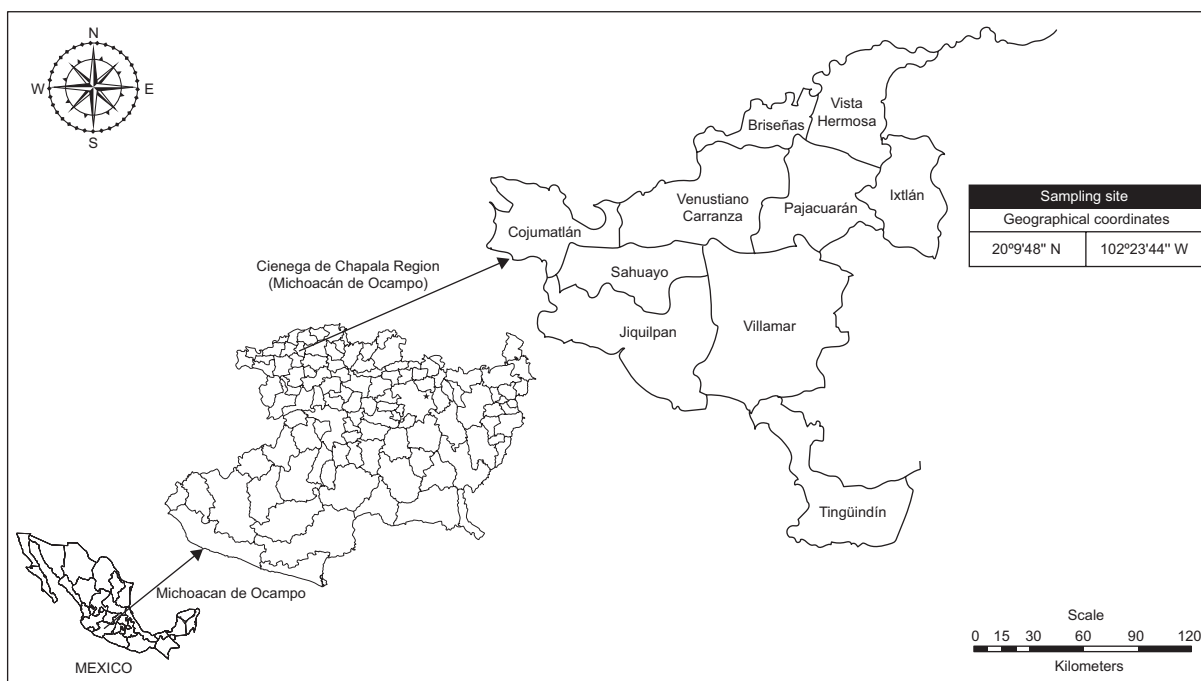


Fig. 1. Location of groundwater sampling collection from Ixtlán de los Hervores, Michoacán, Mexico.

conductivity, temperature and total dissolved solids were measured. The samples were kept at 4 °C until their chemical analysis.

For the groundwater analysis, pH, electric conductivity, temperature and total dissolved solids (TDS) were measured using a Hanna potentiometer model H198129. The concentration of ions present in the groundwater samples was determined by standard methods (Eaton et al. 2005): carbonates and bicarbonates by H_2SO_4 titration; sulphates by BaCl_2 precipitation; chlorides by AgNO_3 precipitation; phosphorus by the persulfate method, and calcium, magnesium, sodium and potassium with a Perkin Elmer 3100 spectrophotometer. The boron concentration was determined by colorimetry using the azomethine-H method and a UV-vis spectrometer (420 nm) (Rodier et al. 2011).

Evaluation of boron adsorption on modified zeolites

The evaluation of boron removal on modified zeolites was performed using: (a) a boron solution prepared by dissolution of boric acid in deionized water, labeled as synthetic boron solution, and (b) groundwater from the well of Ixtlán de los Hervores, Michoacán, Mexico. A solution of boric acid with (5 mg/L) was prepared as synthetic boron solution.

The boron adsorption was carried out in a batch system, where 50 mL of the boron source either synthetic (5 mg/L) or groundwater (5.56 mg/L) were added to an Erlenmeyer flask, then 1 g (pH experiments) or the selected amount (zeolite dosage experiments) of modified zeolite was added. The slurry was kept under stirring at 25 °C for 24 h. Afterwards the solid was recovered, filtered and dried at 40 °C for 24 h. The boron residual concentration in the solution was determined by the azomethine-H method (Rodier et al. 2011). The experiments were performed by triplicate for the trials using groundwater, while for the trials using synthetic boron the experiments were carried out by duplicate.

The adsorbed boron was calculated as follows:

$$\%B_{\text{ads}} = \left(\frac{C_i - C_f}{C_i} \right) \times 100 \quad (1)$$

where $\%B_{\text{ads}}$ is the percentage of adsorbed boron onto zeolite; and C_i and C_f are the initial and final boron concentrations in the solution (mg/L), respectively.

Effect of pH and zeolite dosage on boron removal

To evaluate the effect of pH on the boron adsorption capacity of modified zeolites, the pH of the groundwater (boron concentration = 5.56 mg/L; **Table I**) was adjusted to pH values of 7, 8.5 and 10

TABLE I. CHEMICAL COMPOSITION OF GROUNDWATER USED IN BORON ADSORPTION EXPERIMENTS.

Variable	Unit	Value
pH		7.14
Electrical conductivity	$\mu\text{S/cm}$	1450
Temperature	$^{\circ}\text{C}$	47.5
PO_4^{3-}	mg/L	6.88
B	mg/L	5.56
HCO_3^-	meq/L	3.23
Cl^-	meq/L	5.97
SO_4^{2-}	meq/L	4.09
Ca^{2+}	meq/L	0.82
Mg^{2+}	meq/L	0.56
Na^+	meq/L	10.56
K^+	meq/L	0.74

using NaOH and HNO_3 1M. The modified zeolite was added to groundwater and kept under stirring at 25 $^{\circ}\text{C}$ for 24 h. Afterwards, the residual boron concentration was determined. The optimum pH was selected considering the highest boron removal on each modified zeolite. At this pH, three different zeolite dosage were evaluated: 5, 10 and 20 g/L. The conditions of these trials were carried out at 25 $^{\circ}\text{C}$ for 24 h.

Characterization techniques

The zeolites were analyzed by X-ray diffraction (XRD) using a PANalytical X-ray diffractometer with a $\text{CuK}\alpha$ radiation source ($\lambda = 1.5406 \text{ \AA}$). The transmission electronic microscopy (TEM) (JEOL 1010 field emission microscope, operated at 80 kV) and scanning electronic microscopy (SEM) (JEOL scanning electron microscope, model JSV-6610LV), were used to determine the particle size and morphology of the zeolites, respectively. The particle size distribution was performed using ImageJ software. The textural properties of the zeolites were determined by nitrogen physisorption using Micromeritics ASAP 2010 equipment. The specific surface area was calculated by the Brunauer-Emmett-Teller (BET) method in the relative pressure range ($0.05 < P/P^{\circ} < 0.3$), the total pore volume being obtained at $P/P^{\circ} = 0.99$. Microporous and external surface areas were obtained using the t-plot method. The modified zeolites were analyzed by FT-IR using a Frontier model PerkinElmer spectrophotometer.

Statistical analysis

For the adsorbed boron and zeolite dosage, analysis of variance (ANOVA) and Tukey test were conducted to select the best treatment and mean comparison.

RESULTS AND DISCUSSION

Physical and chemical characterization of the zeolites

From the X-ray diffraction (XRD) patterns of the X (**Fig. 2a**) and LTL (**Fig. 2d**) zeolites it can be observed that both of them were obtained as unique crystalline phases. The X zeolite was identified as faujasite type X (JCPDS 39-0218), while the LTL zeolite was identified as Linde Type L (JCPDS 043-05060). Regarding their textural properties, the zeolites presented adsorption isotherms (**Fig. 2b, e**) corresponding to type IVa. In this kind of isotherm, the capillary condensation occurs, and the hysteresis is observed. This behavior is due to the interactions between the adsorbent and adsorbate as well as the interactions between the molecules in the condensed state (Thommes et al. 2015). Differences were observed in the hysteresis loops of the synthesized zeolites' isotherms. The LTL zeolite exhibited a hysteresis loop type H1, which is associated to materials with a narrow range of mesopores or due to pores of ink-bottle geometry. On the other hand, the X zeolite presented type an H3 hysteresis loop corresponding to non-rigid aggregates of plate-like particles. The pore size distribution of the zeolitic materials is depicted in **figure 2c, f**. It is observed that the X zeolite presented a bimodal distribution in the range of micro and mesopores, whereas for the LTL zeolite its pore size distribution was narrower belonging to the mesopores range.

The textural properties of the zeolites are summarized in **table II**. It was observed that the X zeolite presented a lower specific surface area compared to other reports (Medina-Ramírez et al. 2018, 2021). This behavior can be attributed to the low Si/Al ratio (1.39) of the synthesized X zeolite. According to Shirazi et al. (2008) the BET area is increased as the Si/Al increase. In agreement with the pore size distribution, the X zeolite exhibited a mesoporous area corresponding to 68 % of the total specific surface area. In contrast, the LTL zeolite presented a higher specific surface area, which was mesoporous. Additionally, the average pore size of the LTL zeolite was larger than in the X zeolite. The difference in textural properties of the evaluated zeolites is associated with their topologies, which possess specific building units that determine the type and dimensions of the cavities of the zeolite structure. Particularly, the X zeolite possesses a framework constituted by a sodalite-type cage and a supercage of double 12-member rings. Even though the LTL zeolite presents a similar supercage,

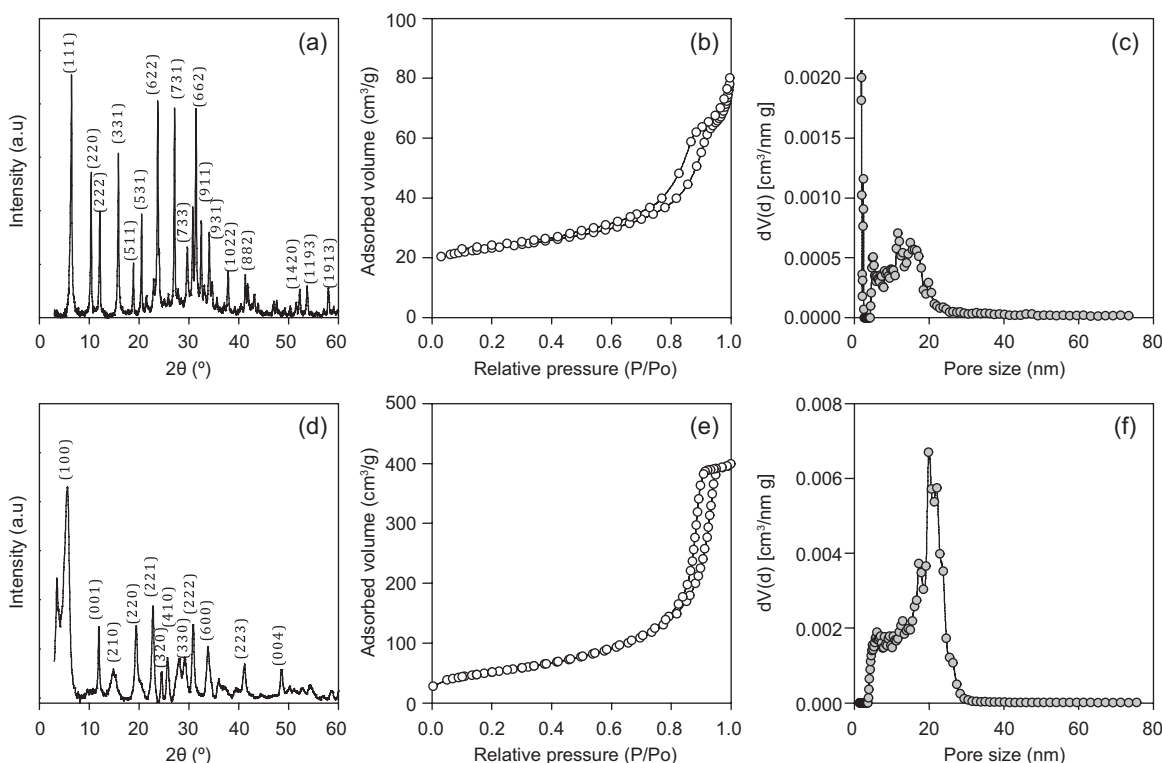


Fig. 2. X-ray diffraction patterns, nitrogen adsorption isotherms and pore size distribution of the (a, b, c) X (FAU X) and (d, e, f) LTL (Linde type L) zeolites. au: area unit; dv(d): derivative of pore volume with respect to pore diameter.

TABLE II. TEXTURAL PROPERTIES OF THE X AND LTL ZEOLITES.

	Si/Al*	SSA (m ² /g)	S _{Micro} (m ² /g)	S _{Meso} (m ² /g)	Total pore volume (cm ³ /g)	V _{Micro} (cm ³ /g)	V _{Meso} (cm ³ /g)	Average pore size (nm)
X zeolite	1.39	57.18	18.14	39.04	0.1242	0.0094	0.1148	6.59
LTL zeolite	2.95	181.6	-	181.6	0.6195	-	0.6195	13.64

*Si/Al: Si and Al ratio, SSA: specific surface area, S_{Micro}: microporous area, S_{Meso}: mesoporous area, V_{Micro}: microporous volume, V_{Meso}: mesoporous volume.

it exhibits a cancrinite-type cage. Additionally, the particle size of the zeolite influenced on its pore size distribution. LTL was obtained as nanocrystals while the X zeolite presented crystals in the range of microns. The presence of nanoparticles enhances the formation of mesopores (2 nm < pore size < 50 nm) and increases the specific surface area.

The morphology of the X and LTL zeolite is depicted in **figure 3**. The X zeolite presented crystalline agglomerates, although the characteristic morphology of this zeolitic phase is octahedral crystals (Parsapur and Selvam 2018). The variation on batch composition and the synthesis led to different morphology. The particle size distribution indicated

that the X zeolite exhibited a size in the range of 0.5-2.2 μm .

On the other hand, the LTL zeolite crystals were observed as tablet-like morphology nanocrystals, in accordance with the findings reported by Wong et al. (2012). The particle size distribution of LTL nanocrystals was in the range of 10-120 nm, its average particle size was of 49 nm.

The pristine and modified zeolites were characterized by FT-IR. The spectra are shown in **figure 4**. It can be observed that for the X zeolite (**Fig. 4a**), two bands were identified associated to symmetric and asymmetric stretching vibration of internal tetrahedral at 674 and 962 cm^{-1} , respectively (Byrappa and

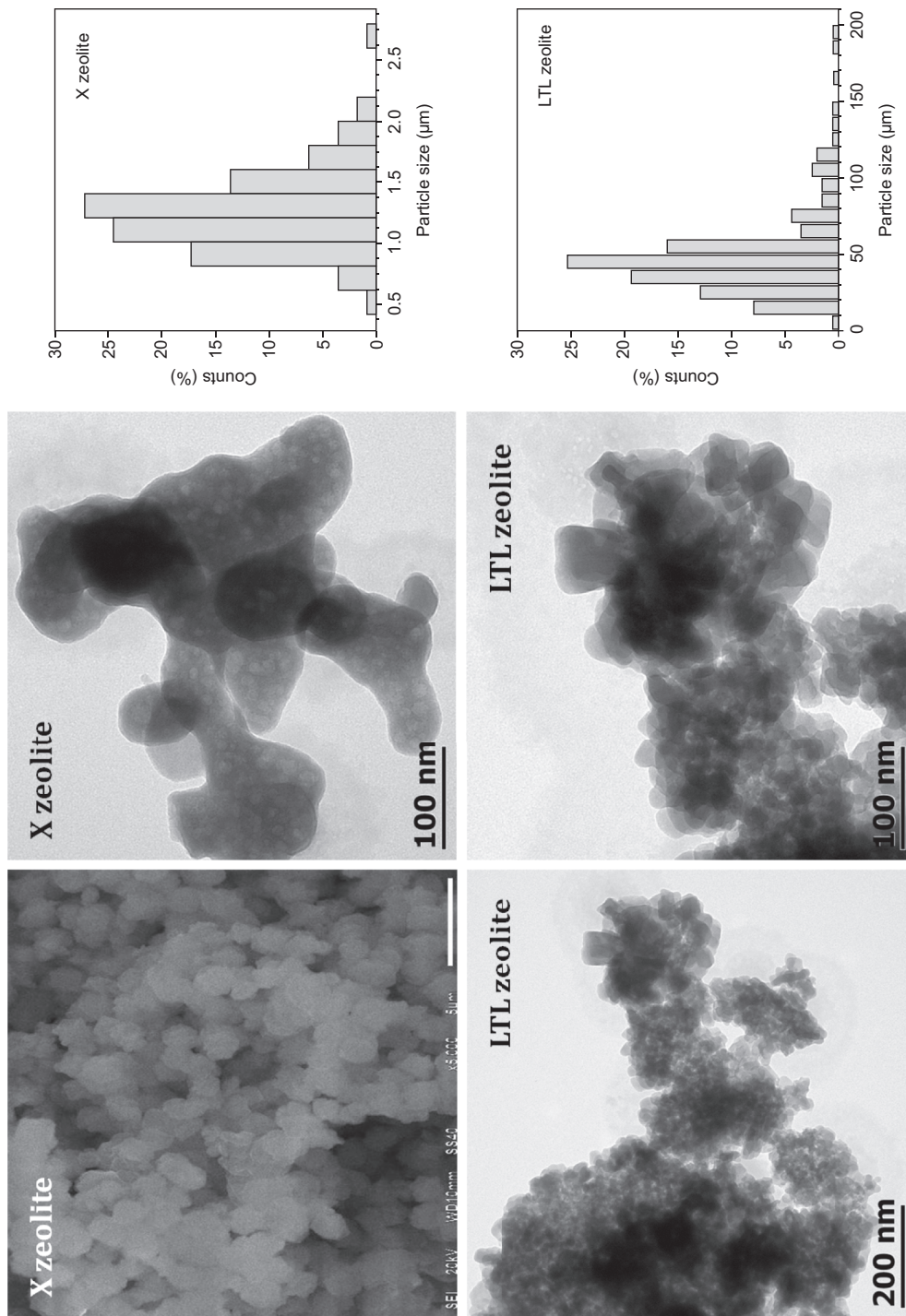


Fig. 3. Scanning electron microscopy and transmission electron microscopy micrographs and particle size distribution of the X (FAU X) and LTL (Linde type-L) zeolites.

Kumar 2007). The T-O bend of internal tetrahedral was attributed to the band at 447 cm^{-1} . Regarding the vibration of the external linkage, the band observed at 674 cm^{-1} corresponded to the symmetric stretching while the band associated to D6R, characteristic of faujasite structures, was detected at a 563 cm^{-1} ,

which is closer to that reported in the literature (November et al. 2011). The presence of adsorbed water on the zeolitic structure was observed around to 1640 cm^{-1} . With respect to the LTL zeolite (Fig. 4b), the asymmetric stretching of the Si-O-T (T = Si, Al) tetrahedral was associated to a band at 1094 and

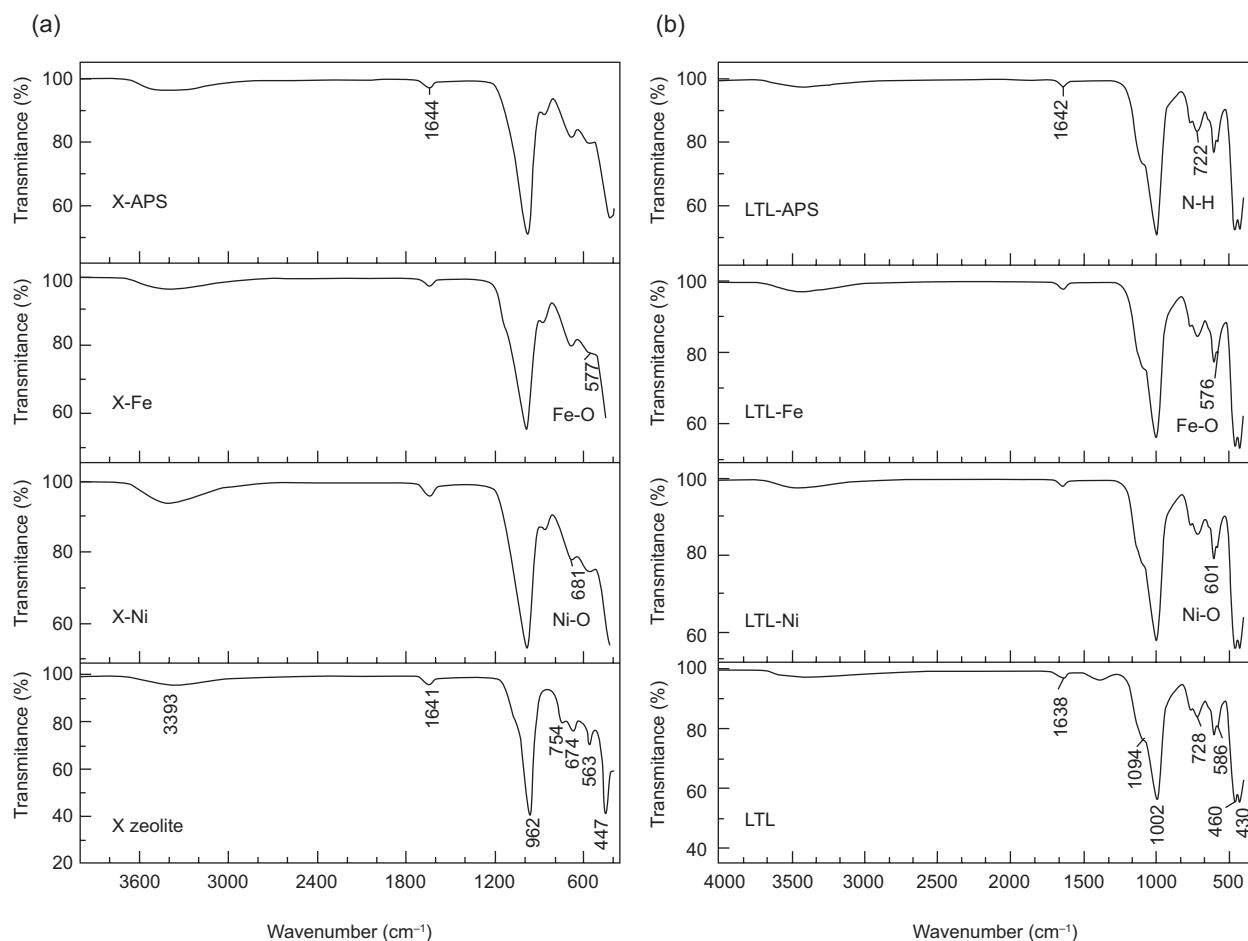


Fig. 4. Fourier transform infrared spectroscopy spectra of the pristine and modified (a) X (FAU X) and (b) LTL (Linde type-L) zeolites.

1002 cm^{-1} (Mozgawa et al. 2011) while the external symmetrical stretching of tetrahedral groups was attributed to the band at 728 cm^{-1} . The presence of double six-member ring was detected at 586 cm^{-1} . The T-O bending and pore opening were associated to the band at 460 and 435 cm^{-1} , respectively (Byrappa and Kumar 2007). For modified zeolites, a slight displacement of the X and LTL zeolite characteristic bands to a lower wavenumber, as well as a decrease in its intensity, were observed. This behavior is due to the difference in ionic radii and occupied sites by the exchanged ions (Krol et al. 2021).

Additionally, bands associated with these ions were identified in zeolites modified with Ni, Fe and APS. Ni was associated with the presence of a Ni-O stretching vibration mode in the region of 600-700 cm^{-1} (Quiao et al. 2009); these bands were observed at 681 cm^{-1} for X-Ni (**Fig. 4a**) and 601 cm^{-1} for LTL-Ni zeolites (**Fig. 4b**). The presence of iron was associated to

the band around 579 cm^{-1} , which corresponds to the Fe-O stretching vibrational mode (Zhang et al. 2017). For the APS modifier, the bands corresponding to the amine group vibration are reported around 1650-1560 cm^{-1} (N-H deformation vibrations) and 3500-3300 cm^{-1} (N-H stretching bands) (Heacock and Marion 2017); however, these regions were overlapped with the bands attributed to the stretching vibration of water molecules (4000-3000 cm^{-1}) and the signals corresponding to bending vibration water (1700-1500 cm^{-1}) in the zeolites (Byrappa and Suresh 2007), so it was not possible to identify them.

Figure 5 shows the SEM micrographs and energy dispersive spectroscopy (EDS) spectra of the modified zeolites. After modification treatment the morphology of the zeolites did not present relevant changes. The presence of Fe and Ni in the zeolites modified with FeCl_3 and NiCl_2 , respectively, was detected by EDS, indicating the effectiveness of the

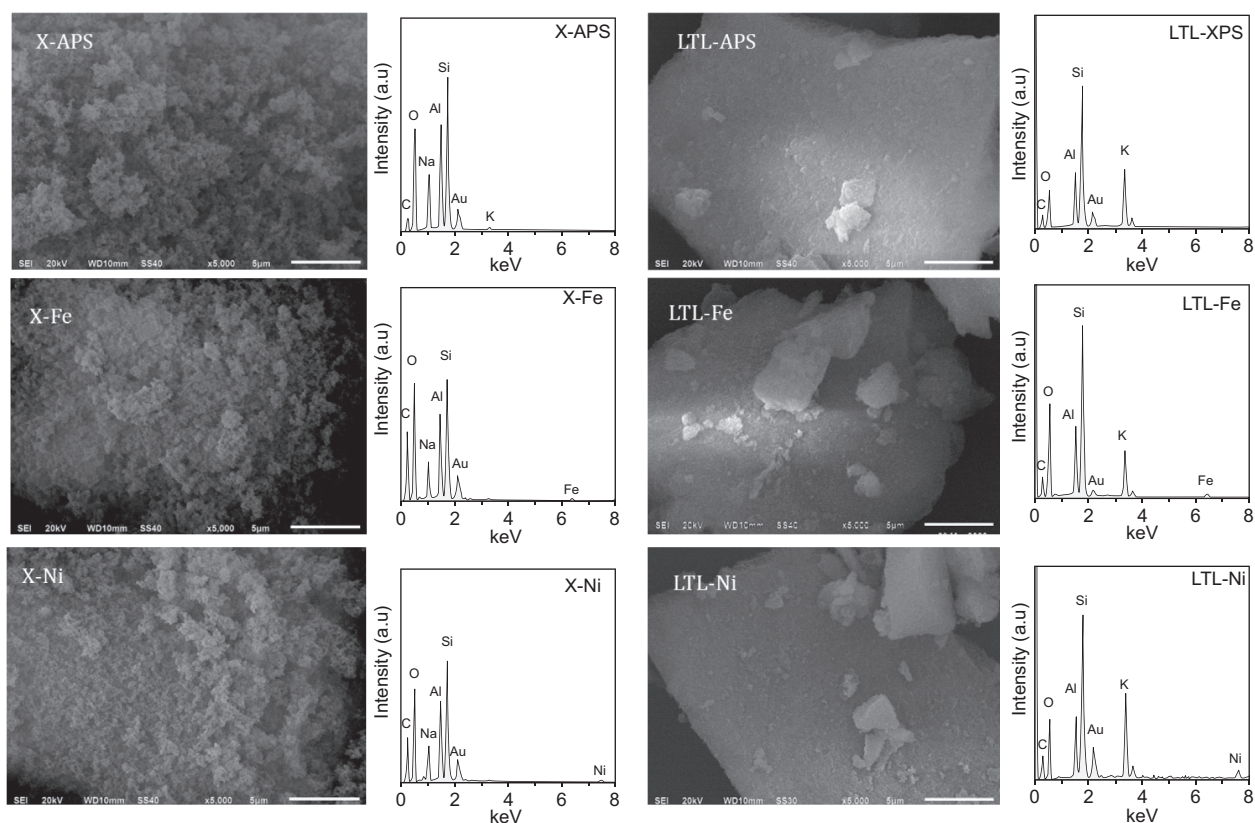


Fig. 5. Scanning electron microscope micrographs and energy dispersive spectroscopy spectra of the modified X (FAU X) and LTL (Linde type-L) zeolites.

ionic exchange. This was corroborated to observe a decrease in the content of sodium in the X zeolite and in potassium content in the LTL zeolite (**Table III**). Additionally, the modification treatment led to an increase in the Si/Al ratio for modified X zeolites, a behavior associated to a dealumination process during the modification (Sato et al. 2003). In contrast, the Si/Al for modified LTL zeolites exhibited slight

variations and these findings can be related to the fact that the pristine LTL zeolite possesses a higher Si/Al ratio than the pristine X zeolite, which conferred to the former a higher structural stability at the modification treatment conditions. On the other hand, the difference on the iron and nickel content of the modified zeolites is associated to the number and accessibility of additional framework sites of

TABLE III. CHANGES IN THE COMPOSITION OF THE MODIFIED ZEOLITES (TOTAL WEIGHT %).

Sample	Si/Al	Na	Fe	Ni	Sample	Si/Al	K	Fe	Ni
X zeolite	1.39	12.44	-	-	LTL zeolite	2.95	19.00	-	-
X-APS	1.67	10.56	-	-	LTL-APS	3.01	19.48	-	-
X-Fe	1.62	9.40	1.96	-	LTL-Fe	2.82	12.00	1.26	-
X-Ni	1.67	8.30	-	2.63	LTL-Ni	2.97	18.05	-	5.16

X zeolite: X zeolite without modification, X-APS: X zeolite modified with aminopropyltriethoxysilane (APS), X-Fe: X zeolite modified with FeCl_3 , X-Ni: X zeolite modified with NiCl_2 ; LTL zeolite: LTL zeolite without modification, LTL-APS: LTL zeolite modified with APS, LTL-Fe: LTL zeolite modified with FeCl_3 , LTL-Ni: LTL zeolite modified with NiCl_2 .

these topologies as well as the ionic radius of the exchanged ions.

Boron adsorption

Figure 6 shows the boron adsorption removal on the modified zeolites, using a synthetic boron solution and groundwater samples at different pH values. As can be observed, all the modified zeolites achieved their highest boron adsorption capacity when the synthetic boron solution was used. Nevertheless, the boron removal capacity on the modified zeolites was reduced when the groundwater was evaluated. This effect was influenced by the zeolite framework and the modifier agent, which are susceptible to the pH and electric conductivity generated by the presence of other chemical species. Regarding the X zeolite, the boron adsorption was higher in the synthetic solution compared to the LTL zeolite; the opposite case was observed in groundwater solutions where the highest adsorption occurred in the LTL zeolite.

It was observed that the equilibrium pH (final pH) increased in the synthetic and groundwater solutions. Shevade and Ford (2004) observed that surface protonation-dissociation reactions of the zeolitic materials can play an important role in the final pH in this kind of experiments. In synthetic solutions, the LTL-APS and X-APS zeolites generated $\text{pH} > 9$, while LTL and X zeolites modified with NiCl_2 and FeCl_3 generated $\text{pH} < 9.0$ (**Fig. 7**); at the same time, the lowest boron adsorption was observed at $\text{pH} > 9.0$, onto APS modified zeolites. The APS modifier contains amino groups ($-\text{NH}$) and it is known that in acid pH these amino groups on the adsorbent surface are protonated ($-\text{NH}_3^+$), whereas a deprotonation occurs when the pH increases. In this last condition, a greater number of surface negative charges is gener-

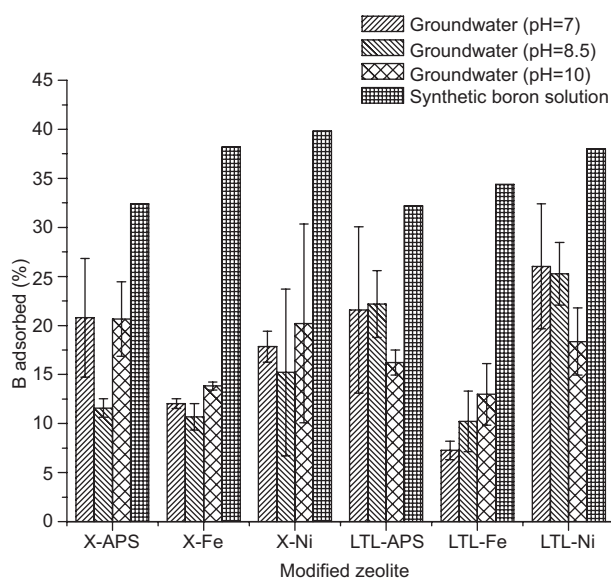


Fig. 6. Boron (B) adsorption on X (FAU X) and LTL (Linde type L) modified zeolites using a synthetic boron solution and groundwater samples at different pH values.

ated (Hozhabr et al. 2015). On the other hand, at $\text{pH} > 9.0$ the main chemical species of boron is $\text{B}(\text{OH})_4^-$, therefore the lower boron adsorption observed at $\text{pH} > 9.0$ can be attributed to an electrostatic repulsion between particles (Irawan et al. 2011, Wei et al. 2011, Adeyemi and Gazi 2016).

In groundwater solutions, the final pH varied depending of the initial pH and type of modified zeolite (**Fig. 8**). As in synthetic boron solutions, the highest final pH was observed on APS modified zeolites (X-APS, LTL-APS).

It is known that pH controls adsorption in the

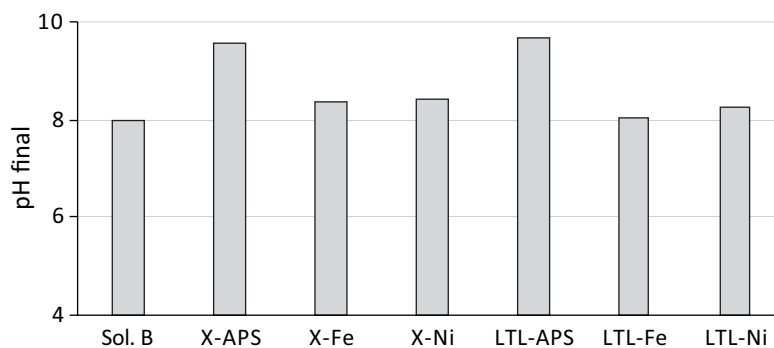


Fig. 7. Final pH (equilibrium pH) of synthetic boron solutions and six modified zeolites. Sol. B: pH of the boron synthetic solution without zeolites; X-APS, X-Fe, X-Ni, LTL-APS, LTL-Fe, and LTL-Ni: X and LTL zeolites modified with aminopropyltriethoxysilane (APS), FeCl_3 and NiCl_2 , respectively.

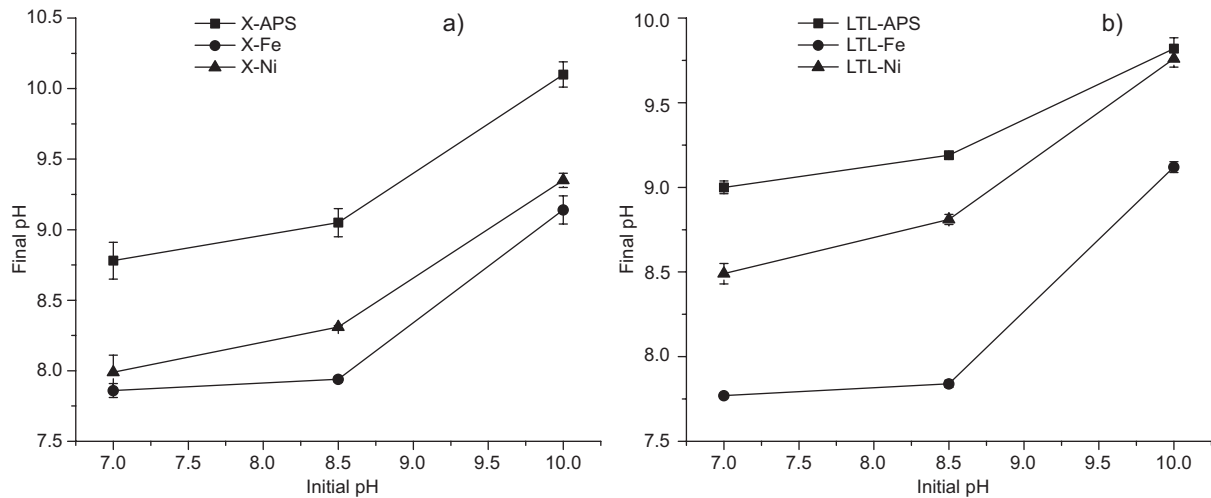


Fig. 8. Change of pH in groundwater solutions at different initial pH values for (a) X (FAU X) and (b) LTL (Linde type L) zeolites.

water interface adsorbent, and it is therefore an important factor in the boron adsorption process (Yuksel and Yurum 2009). The pH also determines the boron chemical species in solution: at low boron concentration (< 25 mM) and $\text{pH} < 9.1$, boron exists mainly as $\text{B}(\text{OH})_3$, while at $\text{pH} > 9.1$, $\text{B}(\text{OH})_4^-$ predominates (Goldberg 1993, Liu et al. 2009, Dionisiou et al. 2013). In this work, the optimal pH values for boron adsorption in both synthetic solutions and groundwater were higher than 8 and less than 9, indicating the presence of the two species of boron (boric acid $\text{B}(\text{OH})_3$ and borates $\text{B}(\text{OH})_4^-$). These pH values are slightly lower than the pK_a of boric acid (9.2), indicating a greater adsorption when this chemical species predominates in the solution (Weidner and Ciesielczyk 2019). Although the chemical species of boron was not determined in this work, according to the boron speciation diagram reported in the literature (Graff et al. 2017) and the concentration of boron for the synthetic solution and groundwater samples used (5 mg/L), as well as the pH evaluated ($\text{pH} = 8\text{--}9$), it was assumed that the species to be removed by the zeolites were borates and boric acid.

Effect of electrical conductivity

Figure 9 shows the relationship of saline concentration, measured as electrical conductivity (EC) in equilibrium solutions and adsorbed boron onto modified zeolites using: (a) a synthetic boron solution and (b) groundwater at three pH values. The EC ranged from 168.6 to 269.1 $\mu\text{S}/\text{cm}$ in the synthetic solution and from 1588 to 2153 $\mu\text{S}/\text{cm}$ in groundwater solu-

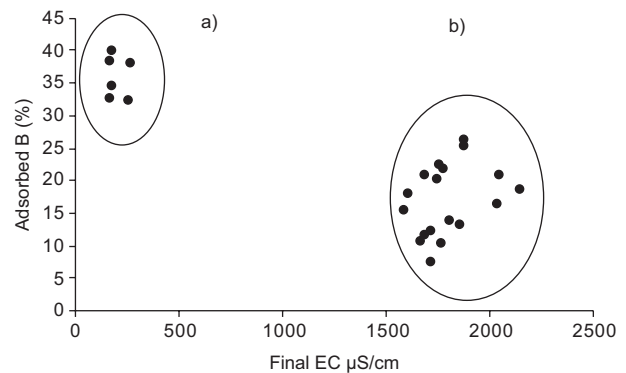


Fig. 9. Ratio of adsorbed boron (%) and final electrical conductivity (EC) in (a) synthetic and (b) groundwater solutions.

tions. Correlation was highly significant $r = -0.829$, $R^2 = 0.687$), showing an inverse relationship between EC and adsorbed boron. The decrease in adsorbed boron with the increase in saline concentration has been explained as a result of the compression of the diffuse double layer between the adsorbent and the surrounding ion solution, which reduces adsorption sites for boron (Adeyemi and Gazi 2016). On the other hand, the ionic strength has also been related to the bond type established between the chemical boron species and the adsorbent. This property has been used to distinguish between inner-sphere complexes, with strong covalent bonds and low dependence of boron adsorption of ionic strength, and external sphere complexes with weaker bonds (hydrogen bridges, electrostatic interactions or hydrophobic

attraction) and high dependence of boron adsorption on the ionic strength of the solution (Goldberg 2005, Liu et al. 2009). The decrease in adsorbed boron with increase in electric conductivity observed in this work (Fig. 9) could indicate that boron interactions with modified zeolites are specific to the type of modifier, therefore the chemical species present influencing its selectivity.

Effect of ions

The ions present in the solutions influence boron adsorption. In this work, the groundwater used is Na-HCO₃, and Na⁺, Cl⁻, SO₄²⁻ and HCO₃⁻ ions predominate (Table I). The anions Cl⁻, SO₄²⁻ and HCO₃⁻ contribute to a lower boron adsorption by competing for adsorption sites onto modified zeolites. This adverse effect of saline ions such as sulfate, chloride, nitrate and carbonate on boron adsorption has been observed by Nasef et al. (2014) onto exchange resins, where the originally adsorbed boron was quickly replaced by the anions present in the solution. However, Senkal and Bicak (2003) mentioned that cations Ca²⁺ and Mg²⁺ do not exert significant interference in boron adsorption when using the iminodipropylene glycol polymer for the removal of boron in water.

Effect of the modifier

Regarding the modifier, it was observed that boron adsorption in the synthetic solution followed this order: NiCl₂ > FeCl₃ > APS (Fig. 6). In these low saline solutions, the main factors affecting boron adsorption are pH and the type of bonds between boron species and the modifier. Ni- and Fe-modified

zeolites generated a final pH > 8 and < 9, while APS-modified zeolites produced a final pH > 9.0, which was related to the highest and lowest boron adsorption, respectively. On the other hand, it is known that nickel forms inner-sphere complexes with boron (Weidner and Ciesielczyk 2019) and strong covalent bonds, which favors the selective adsorption of the chemical forms of boron. Boron adsorption has been observed to be unaffected by co-existing salts in a solution when the adsorption mechanism is based on the formation of such complexes (Liu et al. 2009). In the case of FeCl₃, the adsorption mechanism was probably the formation of external sphere complexes (physical adsorption), since saline concentration affected boron adsorption (Fig. 10). External sphere complexes form weaker bonds such as hydrogen bridges, electrostatic attraction, or hydrophobic attraction (Liu et al. 2009).

In regard to the APS modifier, the main factor affecting boron adsorption was the final pH > 9.0, and boron adsorption was not affected by EC. In relation to adsorption mechanisms, the formation of complexes should be considered based on the observations of Liu et al. (2009), who observed that boron adsorption is significantly unaffected by co-existing salts in a solution when the adsorption mechanism is based on the formation of inner-sphere complexes. Other researchers (e.g., Hozhabr et al. 2015) that have studied Cr(VI) ions adsorption onto silica magnetite nanoparticles modified with 3-APS mention that the electrostatic and hydrogen bond interactions between surface functional groups and HCrO₄⁻ ions have an important role in adsorption process. These three adsorption mechanisms (inner-sphere complexes,

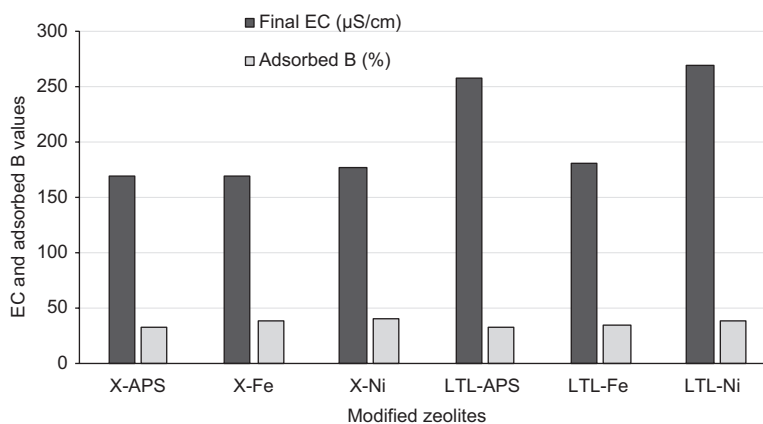


Fig. 10. Final electrical conductivity (EC) and adsorbed boron (B) on six modified zeolites. Synthetic boron solution. X-APS, X-Fe, X-Ni, LTL-APS, LTL-Fe, and LTL-Ni: X (FAU X) and LTL (Linde type L) zeolites modified with aminopropyltriethoxysilane (APS), FeCl₃ and NiCl₂, respectively.

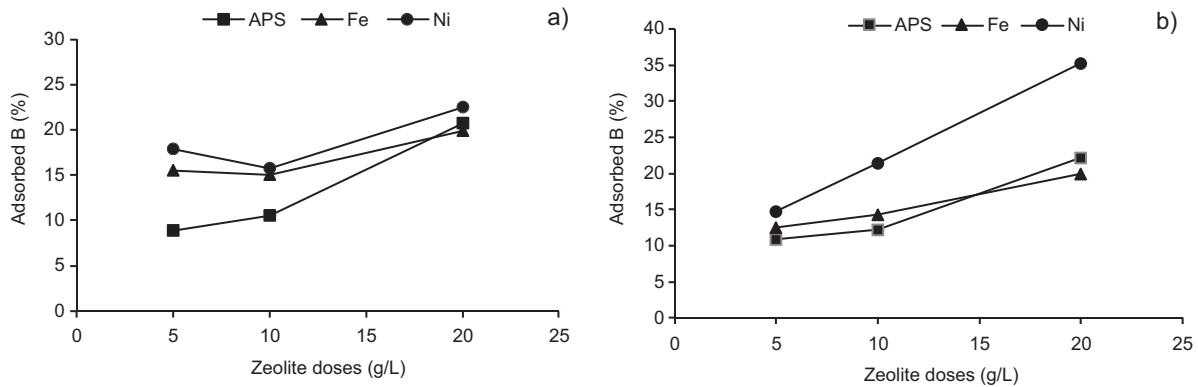


Fig. 11. Adsorbed boron (B) according to modified zeolite concentration. (a) X (FAU X) and (b) LTL (Linde type L) zeolites. Modifiers: APS: aminopropyltriethoxysilane, Fe: FeCl₃, Ni: NiCl₂.

electrostatic and hydrogen bond interactions) could be involved in boron adsorption onto LTL modified zeolites, although more research is required.

Effect of the zeolite dosage

The effect of the dosage of modified zeolite on boron adsorption was tested in three adsorbent concentration (5, 10 and 20 g/L) using groundwater at optimal pH determined for each material. Boron adsorption ranged from 5.6 to 17.9, 10.5 to 21.5 and 16.1 to 35.2 % in adsorbent doses of 5, 10 and 20 g/L, respectively (**Fig. 11**). It is observed that the amount of adsorbed boron was a function of zeolite concentration, an effect derived from increased adsorbent surface area (Demirçivi and Nasün-Saygılı 2010, Demetriou and Pashalidis 2012). The highest percentage of adsorbed boron was obtained with LTL-Ni zeolite at 20 g/L. Because no higher concentrations were explored, it was not possible to determine the maximum adsorption capacity of these modified zeolites, which is suggested to be explored in future research.

The highest boron adsorption onto LTL-Ni zeolites could also be influenced by its textural properties. With regards to the zeolites studied in this work, the specific surface area (SSA), total pore volume, mesoporous area (S_{mes}), mesopore volume (V_{meso}) and average pore size were higher in the LTL zeolite than in the X zeolite (**Table II**). A high specific surface determines, in part, a high adsorption capacity of zeolites by increasing adsorption sites (Batubara et al. 2018), while large cavities or channels in these minerals (identified here by mesopore surface and volume, and mean pore size) were associated with increased ion exchange capacity and molecular adsorption (Byrappa and Yoshimura 2013). In agreement with

these observations, we found that the LTL zeolites exhibited highest average boron adsorption, although only in groundwater solutions with high EC; however, in synthetic boron solutions with low EC, the highest average boron adsorption was obtained with the X zeolite. Both zeolites form type IV isotherms, which are characteristic of multilayer adsorption.

Statistical analysis

The ANOVA for boron adsorption (%) onto six modified zeolites in groundwater solutions with different pH values is shown in **table IV**. Since the probability value (Pr) indicates highly significant differences between treatments, a means separation was performed using the Tukey test ($Pr \leq 0.05$). Results of the Tukey test showed seven groups (**Table V**). Considering the “a” and “ab” groups presented in **table V**, the highest boron adsorption was obtained with LTL-Ni zeolite at pH = 7.0 and LTL-Ni zeolite at pH = 8.5, whereas the LTL-Fe zeolite at pH = 7.0 showed the lowest boron adsorption capacity

TABLE IV. ANOVA FOR BORON ADSORPTION TREATMENTS ON SIX MODIFIED ZEOLITES AND DIFFERENT INITIAL pH VALUES (GROUNDWATER).

Source	F*	SS	AS	F	Pr > F
Model	17	1507.128	88.655	3.99	0.00024
Error	36	799.876	22.219		
Total	53	2307.004			

$R^2 = 0.653$, $R^2_{aj} = 0.490$, RSME (root mean square error) = 4.714.

FD: freedom degrees, SS: sum of squares, AS: average square, F: F value, Pr: probability.

("d" group, **Table V**). For adsorbent dosage, ANOVA indicated highly significant differences between treatments (**Table VI**). For the Tukey mean separation test ($Pr \leq 0.05$), 10 groups were obtained (**Table VII**), where the highest boron adsorption corresponded to LTL-Ni zeolite at a dose of 20 g/L ("a" group, **Table VII**), followed by X-Ni zeolite at 20 g/L ("b" group, **Table VII**).

Comparison of boron adsorption capacity in the six modified zeolites with other materials

The boron adsorption capacity of the modified LTL-Ni zeolite obtained in this work is moderate compared to other materials reported in the literature (**Table VIII**). However, low synthesis costs for these materials are an incentive to continue experimental work on the factors affecting their adsorption and determining the feasibility to using them as effective boron adsorbents. The boron adsorbents considered to be most efficient are exchange and chelating resins (Ipek et al. 2008, Nasef et al. 2014), although they are expensive. Adeyemi and Gazi (2016) used of chitosan as a modifier of the Fe_3O_4 adsorbent in the removal of boron from water, obtaining high values in the adsorption capacity (**Table VIII**).

CONCLUSIONS

Two zeolites (FAU X and LTL) modified with $NiCl_2$, $FeCl_3$ and APS were synthesized and tested for boron adsorption in synthetic and groundwater solutions at different pH and EC. The modified zeolites showed a buffer effect, increasing the final pH in equilibrium solutions. The boron adsorption capacity of zeolites was a function of the pH, EC, and the kind of modifier and adsorbent dosage. The greatest boron adsorption capacity was obtained at $pH > 8$ and < 9 in both solutions, while increased EC in groundwater solutions caused an overall negative effect on boron adsorption. By type of modifier, the best results were obtained with $NiCl_2$ due to its complexing properties with boron species. In groundwater, the zeolitic material with the best response to boron adsorption was the LTL-Ni zeolite at a concentration of 20 g/L, which combines the properties of high surface area, greater volume and mesopore area with the capacity of the $NiCl_2$ modifier to form complexes with boron species. All these characteristics give it the potential use of a selective boron adsorbent. In future research, it is recommended to determine the maximum adsorption capacity of LTL-Ni zeolite,

TABLE V. TUKEY TEST FOR BORON ADSORPTION TREATMENTS ON SIX MODIFIED ZEOLITES AND DIFFERENT INITIAL pH VALUES (GROUNDWATER SOLUTIONS).

Modified zeolite	pH		
	7.0	8.5	10.0
X-APS	20.8 ^{*abcd}	11.6 ^{bcd}	20.7 ^{abcd}
X-Fe	12.03 ^{abcd}	10.7 ^{cd}	13.8 ^{abcd}
X-Ni	17.9 ^{abcd}	15.2 ^{abcd}	20.2 ^{abcd}
LTL-APS	21.6 ^{abcd}	22.2 ^{abc}	16.2 ^{abcd}
LTL-Fe	7.3 ^d	10.2 ^{cd}	19.9 ^{abcd}
LTL-Ni	26.0 ^a	25.3 ^{ab}	18.4 ^{abcd}

X-APS, X-Fe, X-Ni, LTL-APS, LTL-Fe and LTL-Ni: X (FAU X) and LTL (Linde type L) zeolites modified with aminopropyltriethoxysilane (APS), $FeCl_3$ and $NiCl_2$, respectively.

*Averages with different letters are significantly different ($Pr \leq 0.05$), Tukey test.

TABLE VI. ANOVA FOR BORON ADSORPTION TREATMENTS ON SIX MODIFIED ZEOLITES AND THREE ADSORBENT DOSES (5, 10 AND 20 g/L) USING GROUNDWATER.

Source	FD	SS	AS	F	Pr > F
Model	17	1935.981	113.881	16.020	< 0.0001
Error	36	255.918	7.109		
Corrected total	53	2191.899			

$R^2 = 0.883$, $R^2_{aj} = 0.828$, RSME (root mean square error) = 2.666
FD: freedom degrees, SS: sum of squares, AS: average square, F: F value, Pr: probability.

TABLE VII. TUKEY TEST FOR BORON ADSORPTION (%) IN THREE DOSES OF MODIFIED ZEOLITES AND GROUNDWATER.

Modified zeolite	Doses of zeolite		
	5 g/L	10 g/L	20 g/L
X-APS	8.9 ^{*f}	10.5 ^{ef}	20.7 ^{bc}
X-Fe	15.5 ^{bedef}	15.0 ^{bedef}	19.9 ^{bcd}
X-Ni	17.9 ^{bcde}	15.7 ^{bedef}	22.5 ^b
LTL-APS	10.9 ^{ef}	12.3 ^{def}	22.2 ^{bc}
LTL-Fe	12.5 ^{def}	14.3 ^{cdef}	19.9 ^{bcd}
LTL-Ni	14.8 ^{bedef}	21.5 ^{bc}	35.2 ^a

X-APS, X-Fe, X-Ni, LTL-APS, LTL-Fe and LTL-Ni: X (FAU X) and LTL (Linde type L) zeolites modified with aminopropyltriethoxysilane (APS), $FeCl_3$ and $NiCl_2$, respectively.

*Averages with different letters are significantly different ($Pr \leq 0.05$), Tukey test.

TABLE VIII. COMPARATIVE OF MATERIALS WITH DIFFERENT BORON ADSORPTION CAPACITY.

Material	Doses of adsorbent (g/L)	Boron (B) adsorption conditions	Boron adsorption capacity	Reference
LTL-Ni (Linde type L zeolite modified with NiCl ₂)	20	pH = 8.49 T = 25 °C B = 5.5 mg/L	35.2 % (0.216 mg/g)	This work
Fly ash	100	pH = 10.0 T = 25 °C B = 10 mg/L	94 % (0.094 mg/g)	Yüksel and Yürüm (2009)
Demineralized lignite	50	pH = 11.0 T = 25 °C B = 10 mg/L	18 % (0.036 mg/g)	Yüksel and Yürüm (2009)
Clinoptilolite	50	pH = 10.0 T = 25 °C B = 10 mg/L Adsorption time: 24 h	18 % (0.036 mg/g)	Yüksel and Yürüm (2009)
Fe(O)OH	-	pH = 8.0 T = 22 °C B = 55 mg/L	0.03 mol/kg (0.324 mg/g)	Demetriu and Pashalidis (2012)
HFO (hydrous ferric oxide)	-	pH = 9.4 B = 2.25 mM Reaction time: 48 h	1.728 mg/g	Peak et al. (2003)
Al-Fe-Si oxide	25	pH = 8.3 B = 80 mg/L Reaction time: 24 h	0.980 mg/g	Irawan et al. (2011)
Fe ₃ O ₄ -TSPA (bis (trimethoxysilylpropyl)amine)	60	pH = 6.0 T = 22 °C B = 2 M Adsorption time: 2 h	50 mmol/kg (0.5 mg/g)	Liu et al. (2009)
FeO-AC (activated carbon/iron oxide composite)	5	pH = 9.0 B = 80 mg/L Adsorption time = 2 h	97 % (0.485 mg/g)	Chioma et al. (2018)
Polymers VBC (4-vinylbenzylchloride)/DVB (divinyl benzene) + NMDG (N-methyl-D-glucamine)	10	pH = 8.0 T = room temperature B = 350 mg/L Adsorption time = 24 h	18.15 mg/g	Jinging et al. (2018)
Fe ₃ O ₄ -Chitosan-glycidol	5	pH = 7.0 B = 125 mg/L	128.5 mg/g	Adeyemi and Gazi (2016)
Ion exchange resin Diaion CRB 02	2	pH = 8.4 T = 24 °C B = 12-13 mg/L E.C. = 1936 µS/cm	0.31 mmol/g (3.35 mg/g)	Ipek et al. (2008)

as well as to analyze the ability of NiCl₂, FeCl₃ and APS modifiers to react with the surface of zeolites, which may be affecting the adsorption of boron in these materials.

ACKNOWLEDGMENTS

We thank the Instituto Politécnico Nacional and the Universidad de Guanajuato for the financial support and infrastructure for the realization of this work, as well as the Consejo Nacional de Ciencia y Tecnología (CONACyT) for the M.Sc. granted to the first author of this work.

REFERENCES

- Adeyemi O.A. and Gazi M. (2016). Hydroxyl-enhanced magnetic chitosan microbeads for boron adsorption: parameter optimization and selectivity in saline water. *Reactive and Functional Polymers* 109, 23-32. <https://doi.org/10.1016/j.reactfunctpolym.2016.09.005>
- Ayers R.S. and Westcot D.W. (1989). *La calidad del agua y su uso en la agricultura. Estudio FAO riego y drenaje* 29 rev. 1. Food and Agriculture Organization of the United Nations, Rome, Italy, 174 pp.
- Barquist K. and Larsen S.C. (2010). Chromate adsorption on bifunctional, magnetic zeolite composites. *Microporous and Mesoporous Materials* 130 (1-3), 197-202. <https://doi.org/10.1016/j.micromeso.2009.11.005>
- Batubara F., Annisa N. and Turmuzi M. (2018). Nitrate removal using Mg modified zeolite in fluidized-bed system. *Journal of Physics: Conference Series* 1116, 042009. <https://doi.org/10.1088/1742-6596/1116/4/042009>
- Bolt H.M., Basaran N. and Duydu Y. (2020). Effects of boron compounds on human reproduction. *Archives of Toxicology* 94, 717-724. <https://doi.org/10.1007/s00204-020-02700-x>
- Boretti A. and Rosa L. (2019). Reassessing the projections of the World Water Development Report. *NPJ Clean Water* 2 (15), 1-6. <https://doi.org/10.1038/s41545-019-0039-9>
- Byrappa K. and Kummar S.B.V. (2007). Characterization of zeolites by infrared spectroscopy. *Asian Journal of Chemistry* 19, 4933-4935.
- Byrappa K. and Yoshimura M. (2013). Hydrothermal synthesis and growth of zeolites. In: *Handbook of hydrothermal technology* (Byrappa K. and Yoshimura M., Eds.). 2nd ed. Elsevier, Oxford, UK, 315-414.
- Chen T., Wang Q., Lyu J., Bai P. and Guo X. (2020). Boron removal and reclamation by magnetic magnetite (Fe₃O₄) nanoparticle: an adsorption and isotopic separation study. *Separation and Purification Technology* 231, 115930. <https://doi.org/10.1016/j.seppur.2019.115930>
- Chioma A.A., Chung W., Seyam M.A.B., Anak Ch.A.F., Anak J.L.S. and Evuti A.M. (2018). Preparation, characterization and adsorption study of granular activated carbon/iron oxide composite for the removal of boron and organics from wastewater. *E3S Web of Conferences* 34, 02006. <https://doi.org/10.1051/e3sconf/20183402006>
- Demetriou A. and Pashalidis I. (2012). Adsorption of boron on iron-oxide in aqueous solutions. *Desalination and Water Treatment* 37 (1-3), 315-320. <https://doi.org/10.1080/19443994.2012.6612>
- Demirçivi P. and Nasün-Saygili G. (2010). Removal of boron from waste waters using HDTMA-modified zeolites. *Desalination and Water Treatment* 23 (1-3), 110-117. <https://doi.org/10.5004/dwt.2010.1957>
- Dionisiou N.S., Matsi I.T. and Misopolinos N. D. (2013). Removal of boron by surfactant modified zeolitic tuff from Northeastern Greece. *Journal of Agricultural Science* 5 (12), 94-99. <https://doi.org/10.5539/jas.v5n12p94>
- Eaton A.D., Clesceri L.S., Rice E.W. and Greesberg A.E. (2005). *Standard methods for the examination of water and wastewater*. 21st ed. American Public Health Association, Washington, DC, USA, 1207 pp.
- Ezechi E.H., Isa M.H. and Kutty S.R.B.M. (2012). Boron in produced water: Challenges and improvements. A comprehensive review. *Journal of Applied Science* 12 (5), 402-415. <https://doi.org/10.3923/jas.2012.402.415>
- Goldberg S. (2005). Inconsistency in the triple layer model description of ionic strength dependent boron adsorption. *Journal of Colloid and Interface Science* 285 (2), 509-517. <https://doi.org/10.1016/j.jcis.2004.12.002>
- Graff A., Barrez E., Baranek P., Bachet M.M. and Bénézech P. (2017). Complexation of nickel ions by boric acid or (poly)borates. *Journal of Solution Chemistry* 46, 25-43. <https://doi.org/10.1007/s10953-016-0555-x>
- Guan Z., Lv J., Bai P. and Guo X. (2016). Boron removal from aqueous solutions by adsorption. A review. *Desalination* 383, 29-37. <https://doi.org/10.1016/j.desal.2015.12.026>
- Heacock R. and Marion L. (2017). The infrared spectra of secondary amines and their salts. *Canadian Journal of Chemistry* 34, 1782-1795. <https://doi.org/10.1139/v56-231>
- Hilal N., Kim G.J. and Somerfield C. (2011). Boron removal from saline water: a comprehensive review. *Desalination* 273 (1), 23-35. <https://doi.org/10.1016/j.desal.2010.05.012>

- Hozhabr A.S., Entezari M.H. and Chamsaz M. (2015). Modification of mesoporous silica magnetite nanoparticles by 3-aminopropyltriethoxysilane for the removal of Cr (VI) from aqueous solution. *Microporous and Mesoporous Materials* 218, 101-111. <https://doi.org/10.1016/j.micromeso.2015.07.008>
- Ipek I.Y., Kabay N., Yuksel M., Kirmizisakal Ö. and Bryjak M. (2008). Removal of boron from Balçova-Izmir geothermal water by ion exchange process: Batch and column studies. *Chemical Engineering Communications* 196, 277-289. <https://doi.org/10.1080/00986440802289971>
- Irawan Ch., Liu J.C. and Chih-Chao W. (2011). Removal of boron using aluminum-based water treatment residuals (Al-WTRs). *Desalination* 276 (1-3), 322-327. <https://doi.org/10.1016/j.desal.2011.03.070>
- Jalali M., Rajabi F. and Ranjbar F. (2016). The removal of boron from aqueous solutions using natural and chemically modified sorbents. *Desalination and Water Treatment* 57 (18), 8278-8288. <https://doi.org/10.1080/19443994.2015.1020509>
- Jevtić S., Arčon I., Rečnik A., Babić B., Mazaj M., Pavlović J., Matijašević D., Nikšić M. and Rajić N. (2014). The iron (III)-modified natural zeolitic tuff as an adsorbent and carrier for selenium oxyanions. *Microporous and Mesoporous Materials* 197, 92-100. <https://doi.org/10.1016/j.micromeso.2014.06.008>
- <not cited in the text> Jingjing K., Yakun T., Gao S. and Liu L. (2018). One-dimensional controllable cross-linked polymers grafted with N-methyl-d-glucamine for effective boron adsorption. *New Journal of Chemistry* 42 (14), 11334-11340. <https://doi.org/10.1039/C8NJ00461G>
- Khaliq H., Juming Z. and Ke-Mei P. (2018). The physiological role of boron on health. *Biological Trace Element Research* 186, 31-51. <https://doi.org/10.1007/s12011-018-1284-3>
- Kluczka J., Korolewicz T., Zolotajkin M., Simka W. and Raczek M. (2013). A new adsorbent for boron removal from aqueous solutions. *Environmental Technology* 34 (11), 1369-1376. <https://doi.org/10.1080/09593330.2012.750380>
- Koç C. (2007). Effects on environment and agriculture of geothermal wastewater and boron pollution in Great Menderes Basin. *Environmental Monitoring and Assessment* 125, 377-388. <https://doi.org/10.1007/s10661-006-9378-3>
- Krol M., Kolezynski A. and Mosgawa W. (2021). Vibrational spectra of zeolite Y as a function of ion exchange. *Molecules* 26, 342. <https://doi.org/10.3390/molecules26020342>
- Landi M., Margaritopoulou T., Papadakis I.E. and Araniti F. (2019). Boron toxicity in higher plants: An update. *Planta* 250, 1011-1032. <https://doi.org/10.1007/s00425-019-03220-4>
- Lechert H. and Staelin P. (2001). Linde type X. In: *Verified synthesis of zeolitic materials* (Robson H., Ed.). 2nd ed. Elsevier, Amsterdam, The Netherlands, 150-151.
- Liu H., Qing B., Ye X., Li Q., Lee K. and Wu Z. (2009). Boron adsorption by composite magnetic particles. *Chemical Engineering Journal* 151 (1-3), 235-240. <https://doi.org/10.1016/j.cej.2009.03.001>
- Medina-Ramírez A., Gamero-Melo P., Almanza-Robles J.M., Sánchez-Castro M.E., Khamkure S. and García de León R. (2013). Kinetic and thermodynamic study of arsenic (V) adsorption on P and W aluminum functionalized zeolites and its regeneration. *Journal of Water Resource and Protection* 5, 58-67. <https://doi.org/10.4236/jwarp.2013.58A009>
- Medina-Ramírez A., Ruiz-Camacho B., Villicaña-Aguilera M., Galindo-Esquivel I.R. and Ramírez-Minguela J.J. (2018). Effect of different zeolite as Pt supports for methanol oxidation reaction. *Applications of Surface Science* 456, 204-214. <https://doi.org/10.1016/j.apusc.2018.06.105>
- Medina-Ramírez A., Gamero-Melo P., Ruiz-Camacho B., Minchaca-Mojica J.I., Romero-Toledo R. and Gamero-Vega K.Y. (2019). Adsorption of aqueous As (III) in presence of coexisting ions by a green Fe-modified W zeolite. *Water* 11 (281), 1-17. <https://doi.org/10.3390/w11020281>
- Medina-Ramírez A., Trejo-García A.J., Ruiz-Camacho B., López-Badillo C.M., Minchaca-Mojica J.I. and Martínez-Gómez C. (2021) Simple synthesis of hierarchically structured X zeolite from geothermal nanosilica and its evaluation in the dehydration of aqueous solutions of ethanol. *Chemical Papers* 75, 337-349. <https://doi.org/10.1007/s11696-020-01302-2>
- Mintova S. (2016). LTL nanozeolite. In: *Verified synthesis of zeolitic materials* (Mintova S., Ed.). 3rd. revised edition. Synthesis Commission of the International Zeolite Association, Caen, France, 274-275.
- Mosgawa W., Krol M. and Barcik K. (2011). FT-IR studies of zeolites from different structural groups. *Chemik* 6, 671-674.
- Nasef M.M., Nallappan M. and Ujang Z. (2014). Polymer-based chelating adsorbents for the selective removal of boron from water and wastewater: a review. *Reactive and Functional Polymers* 85, 54-68. <https://doi.org/10.1016/j.reactfunctpolym.2014.10.007>
- Noroozifar M., Khorasani-Motlagh M. and Naderpour H. (2014). Modified nanocrystalline natural zeolite for adsorption of arsenate from wastewater: Isotherm and kinetic studies. *Microporous and Mesoporous*

- Materials 197, 101-108. <https://doi.org/10.1016/j.micromeso.2014.05.037>.
- Novembre D., Di Sabatino B., Gimeno D. and Pace C. (2011). Synthesis and characterization of Na-X, Na-A and Na-P zeolites and hydroxysodalite from metakaolinite. *Clay Minerals* 46 (3), 339-354. <https://doi.org/10.1180/claymin.2011.046.3.339>
- Palmucci W. and Rusi S. (2014). Boron-rich groundwater in Central Eastern Italy: A hydrogeochemical and statistical approach to define origin and distribution. *Environmental Earth Science* 72, 5139-5157. <https://doi.org/10.1007/s12665-014-3384-5>
- Parsapur T.K. and Selvam P. (2018). Rational design, synthesis, characterization and catalytic properties of high-quality low-silica hierarchical FAU- and LTA-type zeolites. *Scientific Reports* 8, 16291. <https://doi.org/10.1038/s41598-018-34479-4>
- Peak D., Luther G.W. and Sparks D.L. (2003). ATR-FTIR spectroscopic studies of boric acid adsorption on hydrous ferric oxide. *Geochimica et Cosmochimica Acta* 67 (14), 2551-2560. [https://doi.org/10.1016/S0016-7037\(03\)00096-6](https://doi.org/10.1016/S0016-7037(03)00096-6)
- Price C.J., Marr M.C., Myers C.B., Seely J.C., Heindel J.J. and Schwetz B.A. (1996). The developmental toxicity of boric acid in rabbits. *Fundamental and applied Toxicology* 34 (2), 176-187. <https://doi.org/10.1006/faat.1996.0188>
- Quiao H., Wei Z., Hua Y., Zhu L. and Yan X. (2009). Preparation and characterization of NiO nanoparticles by anodic arc plasma method. *Journal of Nanomaterials* 2009, 795928. <https://doi.org/10.1155/2009/795928>
- Rodier J., Legube B. and Merlet N. (2011). *Análisis del agua*. 9^a ed. Ediciones Omega, Barcelona, España, 1539 pp.
- Sato K., Nishimura Y., Matsubayashi N., Imamura M. and Shimada H. (2003). Structural changes of Y zeolites during ion exchange treatment: Effects of Si/Al ratio of the starting NaY. *Microporous and Mesoporous Materials* 59 (2), 133-146. [https://doi.org/10.1016/S1387-1811\(03\)00305-6](https://doi.org/10.1016/S1387-1811(03)00305-6)
- Schick S., Caillet P., Paillaud J.L., Patarin J. and Mangold-Callarec C. (2010). Batch-wise nitrate removal from water on a surfactant-modified zeolite. *Microporous and Mesoporous Materials* 132 (3), 395-400. <https://doi.org/10.1016/j.micromeso.2010.03.018>
- Senkal B.F. and Bicak N. (2003). Polymer supported iminodipropylene glycol functions for removal of boron. *Reactive and Functional Polymers* 55, 27-33. [https://doi.org/10.1016/S1381-5148\(02\)00196-7](https://doi.org/10.1016/S1381-5148(02)00196-7)
- Shevade S. and Ford R.G. (2004). Use of synthetic zeolites for arsenate removal from pollutant water. *Water Research* 38, 3197-3204. <https://doi.org/10.1016/j.watres.2004.04.026>
- Shirazi L., Jamshidi E. and Ghasemi M.R. (2008). The effect of Si/Al ratio of ZSM-5 zeolite on its morphology, acidity and crystal size. *Crystal Research and Technology* 43 (12), 1300-1306. <https://doi.org/10.1002/crat.200800149>
- Theiss F.L., Ayoko G.A. and Frost R.L. (2013). Removal of boron species by layered double hydroxides: A review. *Journal of Colloid and Interface Science* 402, 114-121 <https://doi.org/10.1016/j.jcis.2013.03.051>
- Thommes M., Kaneko K., Neimark A., Olivier J., Rodríguez-Reinoso F., Rouquerol J. and Sing K. (2015). Physisorption of gases, with special reference to the evaluation of surface area and pore size distribution (IUPAC technical report). *Pure and Applied Chemistry* 87 (9-10), 1051-1069. <https://doi.org/10.1515/pac-2014-1117>
- Velázquez M., Pimentel J.L. and Ortega M. (2011). Estudio de la distribución del boro en fuentes de agua de la cuenca del río Duero, México, utilizando análisis estadístico multivariado. *Revista Internacional de Contaminación Ambiental* 27 (1), 19-30.
- Verbinnen B., Block Ch., Hannes D., Lievens P., Vavclavikova M., Stefusova K., Gallios G. and Vandecasteele C. (2012). Removal of molybdate anions from water by adsorption on zeolite-supported magnetite. *Water Environment Research* 84 (9), 753-760. <https://doi.org/10.2175/106143012x13373550427318>
- Wei Y., Zheng Y. and Chen J.P. (2011). Design and fabrication of an innovative and environmental friendly adsorbent for boron removal. *Water Research* 45 (6), 2297-2305. <https://doi.org/10.1016/j.watres.2011.01.003>
- Weidner E. and Ciesielczyk F. (2019). Removal of hazardous oxyanions from the environment using metal-oxide-based materials. *Materials* 12 (927), 1-32. <https://doi.org/10.3390/ma12060927>
- Weir R.J. and Fisher R.S. (1972). Toxicologic studies on borax and boric acid. *Toxicology and Applied Pharmacology* 23 (3), 351-364. [https://doi.org/10.1016/0041-008X\(72\)90037-3](https://doi.org/10.1016/0041-008X(72)90037-3)
- Wong J.T., Ng E.P. and Adam F. (2012). Microscopic investigation of nanocrystalline zeolite L synthesized from rice husk ash. *Journal of the American Ceramic Society* 95, 805-808. <https://doi.org/10.1111/j.1551-2916.2011.04995.x>
- WHO (2017). *Guidelines for drinking-water quality*. Fourth edition incorporating the first addendum. Manual. World Health Organization, Geneva, Switzerland, 631 pp.
- Xu R., Xing X., Zhou Q., Jiang G. and Wei F. (2010). Investigations on boron levels in drinking water sources in China. *Environmental Monitoring and Assessment* 165, 15-25. <https://doi.org/10.1007/s10661-009-0923-8>

- Xu H., Hashimoto K., Maeda S., Azimi M.D., Fayaz S.H., Chen W., Hamajima N. and Kato M. (2020). High levels of boron promote anchorage-independent growth of nontumorigenic cells. *Environmental Pollution* 266 (115094), 1-7. <https://doi.org/10.1016/j.envpol.2020.115094>
- Yu Ch. and Han X. (2015). Adsorbent material used in water treatment. A review. 2nd International Workshop on Materials Engineering and Computer Sciences, 290-293.
- Yüksel S. and Yürüm Y. (2009). Removal of boron from aqueous solutions by adsorption using fly ash, zeolite, and demineralized lignite. *Separation Science and Technology* 45 (1), 105-115. <https://doi.org/10.1080/01496390903256042>
- Zhang T., Zhao N., Li J., Gong H., An T., Zhao F. and Ma H. (2017). Thermal behavior of nitrocellulose-based superthermites: Effects of nano-Fe₂O₃ with three morphologies. *RSC Advances* 7, 23583-23590. <https://doi.org/10.1039/c6ra28502c>